

Preliminary lattice QCD study of the $I = 1$ $K\bar{K}$ scattering length

Ziwen Fu

Key Laboratory of Radiation Physics and Technology (Sichuan University), Ministry of Education;
Institute of Nuclear Science and Technology; Sichuan University, Chengdu 610064, P. R. China.

The s -wave kaon-antikaon ($K\bar{K}$) elastic scattering length is investigated by lattice simulation using pion masses $m_\pi = 330 - 466$ MeV. Through moving wall sources without gauge fixing, we calculate $K\bar{K}$ four-point correlation functions for isospin $I = 1$ channel in the “Asqtad” improved staggered fermion formulation, and observe a clear signal of attraction, which is consistent with other pioneering lattice studies on $K\bar{K}$ potential. Extrapolating $K\bar{K}$ scattering length to the physical point, we obtain $m_K a_{K\bar{K}}^{I=1} = 0.211(33)$. These simulations are performed with MILC gauge configurations at lattice spacing $a \approx 0.15$ fm.

PACS numbers: 12.38.Gc, 11.15.Ha

I. INTRODUCTION

The elastic $K\bar{K}$ scattering is one of the simplest reactions with strange quark, and it allows for an explicit exploration of the three-flavor hadronic structure. The measurement of $K\bar{K}$ scattering is very useful for our study of the chiral symmetry breaking of quantum chromodynamics (QCD). In the isospin limit, the $K\bar{K}$ system have two isospin eigenstates, namely, $I = 1$ and 0 [1].

During the last decade, the experimental measurements of the $K\bar{K}$ scattering have been carried out at several cooler-synchrotron COSY facilities [2–8]. Because of the high momentum resolution of COSY, the thresholds from neutral and charged kaons are well separated and can be studied independently, and the values of total and differential cross sections are now available for a variety of reactions [2–8], where the prompt K^+K^- spectrum is described by a four-body phase-space distribution, modified by the various final state interaction [2–8]. These results show a clear evidence for the smooth K^+K^- background.

It should be stressed that, based on the low energy K^+K^- invariant mass distributions and generalized Dalitz plot analysis, Silarski et al. first estimated the scattering length for the K^+K^- interaction to be $|Re(a_{K^+K^-})| = 0.5_{-0.5}^{+4.0}$ fm and $Im(a_{K^+K^-}) = 3.0 \pm 3.0$ fm [6]. Later, they improve these results as $|Re(a_{K^+K^-})| = 0.2_{-0.2}^{+0.8}$ fm, $Im(a_{K^+K^-}) = 0.4_{-0.4}^{+0.6}$ fm [9]. Since K^+K^- system is a mixture of the isospin $I = 0$ and 1, in those analyses we can not distinguish between the $I = 0$ and 1 channels.

The determination of $K\bar{K}$ scattering from QCD is very difficult since it is essentially a non-perturbative problem. However, some theoretical efforts are still taken to study the $K\bar{K}$ scattering [10–12]. But, if the scattering hadrons contain strange quarks, the chiral perturbation theory (χ PT) predictions usually suffer from considerable corrections because of the resonances f_0 and a_0 , and one has to apply chiral unitary theory, sometimes called unitarized chiral perturbation theory [13–16].

The most feasible way to extract $K\bar{K}$ scattering length nonperturbatively from first principles is using lattice

QCD. And it offers an another important consistent check of the validity of χ PT with the inclusion of the strange quarks. Although there are some exploratory lattice QCD investigations of the meson anti-meson potential (including $K\bar{K}$ potential) in Refs. [17, 18], until now, no lattice QCD study about its scattering length has been reported, mainly because it is extremely difficult to reliably calculate the rectangular and disconnected diagrams. Motivated by the first lattice study of the s -wave K^+K^+ scattering length in the $I = 1$ channel, which was explored by NPLQCD Collaboration in fully-dynamical lattice QCD with domain-wall valence [19] and the value of $m_K a_{K^+K^+}$ was found to be $-0.352(16)$, we will explore the $K\bar{K}$ scattering length from lattice QCD. This is also encouraged by our reliable extractions of the πK [20, 21] and $\pi\pi$ [22] scattering lengths.

Lüscher [23, 24] established the basic formulae for the calculation of the scattering length using lattice QCD, which is valid for the elastic scattering below inelastic thresholds. Below kinematic thresholds, the scattering length of two hadrons is connected to the energy phase shift of two-hadron state enclosed in a torus. This method paved the way for our lattice calculations of $K\bar{K}$ scattering. We should bear in mind that, above the inelastic threshold, a tower of resonances emerges, which suggest the opening of other channels.

It is well-known that the appearance of the $f_0(I = 0)$ and $a_0(I = 1)$, is due to the introduction of the $K\bar{K}$ scattering channel [1]. They decay mainly into $\pi\pi$ and $\pi\eta$, respectively. Both have the masses around 980 MeV [25]. Since the central mass values fall almost exactly at the $K\bar{K}$ threshold, the strong coupling to this channel distorts significantly the upper parts of the mass spectra.

As presented later, for isospin $I = 0$ channel, we need calculating vacuum diagram, which is extremely difficult to reliably measure. Thus, we here will preliminarily report our lattice simulations on the $K\bar{K}$ scattering length in the $I = 1$ channel. In the presence of the strange quark exchange channel, the $K\bar{K}$ scattering length have imaginary contribution. For instance, the experimental determinations of the scattering lengths are complex as dictated by the various decay channel thresholds [2–8].

The S matrix has the structure

$$S = \begin{bmatrix} \eta e^{2i\delta_{K\bar{K}}} & i(1-\eta^2)^{1/2} e^{i(\delta_{K\bar{K}}+\delta_{\pi\eta})} \\ i(1-\eta^2)^{1/2} e^{i(\delta_{K\bar{K}}+\delta_{\pi\eta})} & \eta e^{2i\delta_{\pi\eta}} \end{bmatrix}$$

where $\delta_{K\bar{K}}$ and $\delta_{\pi\eta}$ are the phase shifts for the elastic $K\bar{K} \rightarrow K\bar{K}$ and $\pi\eta \rightarrow \pi\eta$ processes in isospin $I = 1$ channel and η is the inelasticity. We note that, using $(S)_{11}$ and $(S)_{22}$ we can determine η , $\delta_{K\bar{K}}$ and $\delta_{\pi\eta}$.

We will use the MILC gauge configurations generated with the $N_f = 2 + 1$ flavors of the Asqtad improved [26, 27] staggered dynamical sea quarks [28, 29] to calculate the elastic $K\bar{K}$ phase shift $\delta_{K\bar{K}}$ and then evaluate the s -wave $K\bar{K}$ scattering length for isospin $I = 1$ channel in the absence of resonant states. We adopt the technique introduced in Refs. [30, 31], namely, the moving wall sources without gauge fixing, to obtain the reliable accuracy, and observe a clear signal of attraction, which is consistent with pioneering lattice studies on $K\bar{K}$ potential in Refs. [17, 18]. Moreover, we extrapolate the $K\bar{K}$ scattering length to the physical point using the continuum three-flavor χ PT form at the next-to-leading order (NLO), which are provided in B with the help of Zhi-Hui Guo, and it can be directly built from the its scattering amplitudes in Ref. [32],

This article is organized as follows. In Sect. II, we describe the formalism for the calculation of the $K\bar{K}$ scattering lengths using the Lüscher's formula [23, 24] and our computational technique for $K\bar{K}$ four-point functions. We present our lattice results in Sect. III, and arrive at our conclusion and outlook in Sect. IV.

II. METHOD

Here we follow the original notations and conventions in Refs. [30–34] to review the required formulae for calculating $K\bar{K}$ scattering lengths. In the Asqtad-improved staggered dynamical fermion formalism, let us study the $K\bar{K}$ scattering of one Goldstone kaon and one Goldstone anti-kaon. Using operators $O_K(x_1)$, $O_K(x_2)$ for kaons at lattice points x_1 , x_2 , and operators $O_{\bar{K}}(x_3)$, $O_{\bar{K}}(x_4)$ for anti-kaons at lattice points x_3 , x_4 , respectively, we can express the $K\bar{K}$ four-point correlation function as

$$C_{K\bar{K}}(x_4, x_3, x_2, x_1) = \langle O_{\bar{K}}(x_4) O_{\bar{K}}(x_3) O_K^\dagger(x_2) O_K^\dagger(x_1) \rangle, \quad (1)$$

where the kaon and anti-kaon interpolating field operators are denoted by

$$\begin{aligned} \mathcal{O}_{K^+}(t) &= \sum_{\mathbf{x}} \bar{s}(\mathbf{x}, t) \gamma_5 u(\mathbf{x}, t), \\ \mathcal{O}_{K^0}(t) &= \sum_{\mathbf{x}} \bar{s}(\mathbf{x}, t) \gamma_5 d(\mathbf{x}, t), \\ \mathcal{O}_{\bar{K}^0}(t) &= - \sum_{\mathbf{x}} \bar{d}(\mathbf{x}, t) \gamma_5 s(\mathbf{x}, t), \\ \mathcal{O}_{K^-}(t) &= \sum_{\mathbf{x}} \bar{u}(\mathbf{x}, t) \gamma_5 s(\mathbf{x}, t). \end{aligned} \quad (2)$$

After summing over the spatial coordinates, we achieve the $K\bar{K}$ four-point correlation function,

$$C_{K\bar{K}}(t_4, t_3, t_2, t_1) = \sum_{\mathbf{x}_1} \sum_{\mathbf{x}_2} \sum_{\mathbf{x}_3} \sum_{\mathbf{x}_4} C_{K\bar{K}}(x_4, x_3, x_2, x_1), \quad (3)$$

where $x_1 \equiv (\mathbf{x}_1, t_1)$ (likewise for x_2 , x_3 , and x_4), and t represents the time difference, namely, $t \equiv t_3 - t_1$. We build $K\bar{K}$ operators for two isospin eigenstates as [1]¹

$$\begin{aligned} |K\bar{K}(I=0)\rangle &= \sqrt{\frac{1}{2}} \left\{ |K^+K^- \rangle - |K^0\bar{K}^0 \rangle \right\}, \\ |K\bar{K}(I=1)\rangle &= \sqrt{\frac{1}{2}} \left\{ |K^+K^- \rangle + |K^0\bar{K}^0 \rangle \right\}. \end{aligned}$$

Then, the scattering amplitudes M for $K\bar{K}$ scattering in the $I = 1$ and 0 states are given by

$$\begin{aligned} M(I=1) &= \frac{1}{2} \langle K^+K^- | S | K^+K^- \rangle + \frac{1}{2} \langle K^+K^- | S | K^0\bar{K}^0 \rangle \\ &\quad + \frac{1}{2} \langle K^0\bar{K}^0 | S | K^+K^- \rangle + \frac{1}{2} \langle K^0\bar{K}^0 | S | K^0\bar{K}^0 \rangle, \quad (4) \\ M(I=0) &= \frac{1}{2} \langle K^+K^- | S | K^+K^- \rangle - \frac{1}{2} \langle K^+K^- | S | K^0\bar{K}^0 \rangle \\ &\quad - \frac{1}{2} \langle K^0\bar{K}^0 | S | K^+K^- \rangle + \frac{1}{2} \langle K^0\bar{K}^0 | S | K^0\bar{K}^0 \rangle. \quad (5) \end{aligned}$$

We substitute Eq. (2) into Eq. (1) to obtain the quark diagrams for the $K\bar{K}$ scattering in the $I = 1$ channel. The concrete calculations are given in A for reference. At last, we obtain 12 different diagrams for the $I = 1$ channel, which correspond to Eqs. (A1) - (A12), and are also shown in Figs. 1 and 2,

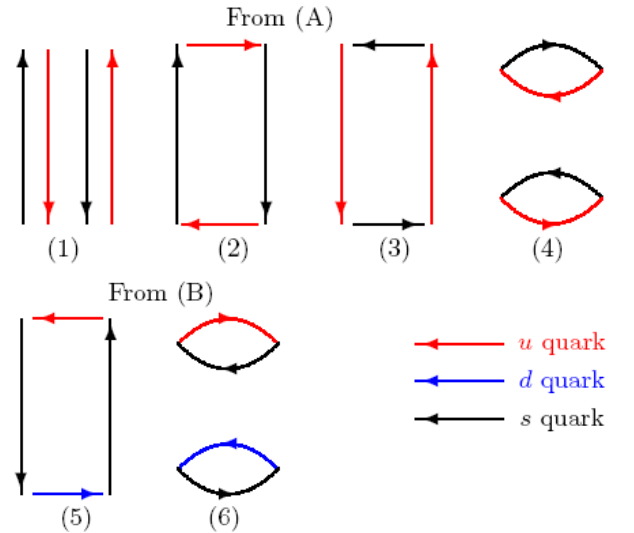


FIG. 1: The numbers below the quark line diagrams correspond to the terms (A1) - (A6) given in Appendix A. (A) and (B) correspond to the first and second terms in Eq. (4), respectively.

¹ Our phase conventions for pseudoscalar mesons are different from those in Ref. [1].

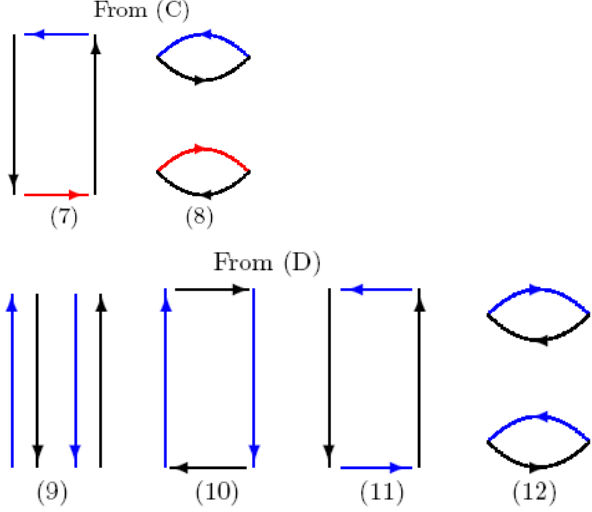


FIG. 2: The numbers below the quark line diagrams correspond to the terms (A7) - (A12) given in Appendix A. (C) and (D) correspond to the third and fourth terms in Eq. (4), respectively.

In the isospin limit, we can classify the 12 quark line diagrams into four independent groups. Diagram 1 in Fig. 1 and diagram 9 in Fig. 2 are categorized into Group 1. Likewise, diagrams 3 and 10 are categorized into Group 2; Nos. 2, 5, 7, and 11 in Group 3; Nos. 4, 6, 8, and 12 in Group 4; respectively. By inspecting Eq. (4) and Eqs. (A1) - (A12), the coefficients of these groups are given as

$$\begin{aligned}
 \text{Group 1:} & \quad \frac{1}{2} + \frac{1}{2} = 1 : D, \\
 \text{Group 2:} & \quad \frac{1}{2}(-1) + \frac{1}{2}(-1) = -1 : R_u, \\
 \text{Group 3:} & \quad \frac{1}{2} + \left(\frac{1}{2}\right)(-1) + \left(\frac{1}{2}\right)(-1) + \frac{1}{2} = 0 : R_s, \\
 \text{Group 4:} & \quad \frac{1}{2} + \left(\frac{1}{2}\right)(-1) + \left(\frac{1}{2}\right)(-1) + \frac{1}{2} = 0 : V,
 \end{aligned} \tag{6}$$

where, R_u , R_s are two types of the rectangular quark diagrams and the subscript u and s distinguish two of them, since for R_u rectangular quark diagram, there are two u quark lines on the time direction, likewise for R_s . At last, only two diagrams still contribute to $K\bar{K}$ scattering amplitudes for the isospin $I = 1$ channel. For the $I = 0$ case, we can easily perform the same procedures. Finally, both channels can be written in terms of the diagrams D , R_u , R_s and V , namely [17, 18]

$$\begin{aligned}
 M(I = 1) &= D - R_u, \\
 M(I = 0) &= D - R_u - 2R_s + 2V.
 \end{aligned} \tag{7}$$

To avert the Fierz rearrangement of quark lines [30, 31], we select $t_1 = 0$, $t_2 = 1$, $t_3 = t$, and $t_4 = t + 1$.

Then, we can build $K\bar{K}$ operators for isospin $I = 1$ and 0 eigenstates as [1]

$$\begin{aligned}
 \mathcal{O}_{K\bar{K}}^{I=0}(t) &= \frac{1}{\sqrt{2}} \left\{ K^+(t)K^-(t+1) - K^0(t)\bar{K}^0(t+1) \right\}, \\
 \mathcal{O}_{K\bar{K}}^{I=1}(t) &= \frac{1}{\sqrt{2}} \left\{ K^+(t)K^-(t+1) + K^0(t)\bar{K}^0(t+1) \right\},
 \end{aligned} \tag{8}$$

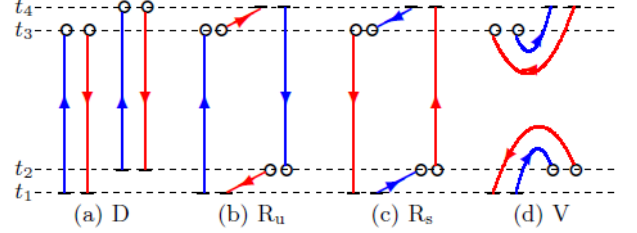


FIG. 3: Diagrams contributing to $K\bar{K}$ four-point functions. Short bars stand for wall sources. Open circles are sinks for local kaon or anti-kaon operators. The blue and red lines represent the u/d and strange quark lines, respectively.

In the isospin limit, four quark line diagrams contribute to the $K\bar{K}$ scattering amplitudes; we plot them in Fig. 3, and label them as direct (D), rectangular (R_u), rectangular (R_s), and vacuum (V) diagrams, respectively. It is pretty easy to evaluate the direct diagram, while the reliable evaluation of the rectangular (R_u , R_s) and vacuum (V) diagrams is extremely difficult [30, 31]. We settle it through the moving wall source technique introduced in Refs. [30, 31], namely, each propagator, which corresponds to a moving wall source at $t = 0, \dots, T - 1$, is denoted by

$$\sum_{n''} D_{n', n''} G_t(n'') = \sum_{\mathbf{x}} \delta_{n', (\mathbf{x}, t)}, \quad 0 \leq t \leq T - 1,$$

where D defines the quark matrix for the quark action. D , R_u , R_s and V are schematically displayed in Fig. 3, and we can also write them in terms of the quark propagators G , namely,

$$\begin{aligned}
 C_D(t_4, t_3, t_2, t_1) &= \sum_{\mathbf{x}_3} \sum_{\mathbf{x}_4} \langle \text{Tr}[G_{t_1}^{(u)\dagger}(\mathbf{x}_3, t_3)G_{t_1}^{(s)}(\mathbf{x}_3, t_3)] \\
 &\quad \times \text{Tr}[G_{t_2}^{(u)\dagger}(\mathbf{x}_4, t_4)G_{t_2}^{(s)}(\mathbf{x}_4, t_4)] \rangle, \\
 C_{R_u}(t_4, t_3, t_2, t_1) &= \sum_{\mathbf{x}_2} \sum_{\mathbf{x}_3} \langle \text{Tr}[G_{t_1}^{(s)\dagger}(\mathbf{x}_2, t_2)G_{t_4}^{(u)}(\mathbf{x}_2, t_2) \\
 &\quad \times G_{t_4}^{(s)\dagger}(\mathbf{x}_3, t_3)G_{t_1}^{(u)}(\mathbf{x}_3, t_3)] \rangle, \\
 C_{R_s}(t_4, t_3, t_2, t_1) &= \sum_{\mathbf{x}_2} \sum_{\mathbf{x}_3} \langle \text{Tr}[G_{t_1}^{(u)\dagger}(\mathbf{x}_2, t_2)G_{t_4}^{(s)}(\mathbf{x}_2, t_2) \\
 &\quad \times G_{t_4}^{(u)\dagger}(\mathbf{x}_3, t_3)G_{t_1}^{(s)}(\mathbf{x}_3, t_3)] \rangle, \\
 C_V(t_4, t_3, t_2, t_1) &= \sum_{\mathbf{x}_2} \sum_{\mathbf{x}_3} \left\{ \langle \text{Tr}[G_{t_1}^{(u)\dagger}(\mathbf{x}_2, t_2)G_{t_1}^{(s)}(\mathbf{x}_2, t_2)] \right. \\
 &\quad \times \text{Tr}[G_{t_4}^{(u)\dagger}(\mathbf{x}_3, t_3)G_{t_4}^{(s)}(\mathbf{x}_3, t_3)] \rangle - \\
 &\quad \langle \text{Tr}[G_{t_1}^{(u)\dagger}(\mathbf{x}_2, t_2)G_{t_1}^{(s)}(\mathbf{x}_2, t_2)] \rangle \\
 &\quad \left. \times \langle \text{Tr}[G_{t_4}^{(u)\dagger}(\mathbf{x}_3, t_3)G_{t_4}^{(s)}(\mathbf{x}_3, t_3)] \rangle \right\}, \tag{9}
 \end{aligned}$$

where we utilize the hermiticity properties of G to remove the γ^5 factors. The vacuum diagram here include a vacuum subtraction term.

According to the discussions in Refs. [30, 31], the $K\bar{K}$ rectangular and vacuum diagrams in Fig. 3 produce the gauge-variant noise, and we will perform the gauge field average without gauge fixing to nicely suppress this noise. We can construct physical $K\bar{K}$ correlators with certain isospin by integrating four types of the propagators. In the isospin limit, we can express the $K\bar{K}$ correlator for isospin $I = 1$ and 0 channels by

$$\begin{aligned} C_{K\bar{K}}^{I=0}(t) &\equiv \langle \mathcal{O}_{K\bar{K}}^{I=0}(t) | \mathcal{O}_{K\bar{K}}^{I=0}(0) \rangle = D - R_u - 2R_s + 2V, \\ C_{K\bar{K}}^{I=1}(t) &\equiv \langle \mathcal{O}_{K\bar{K}}^{I=1}(t) | \mathcal{O}_{K\bar{K}}^{I=1}(0) \rangle = D - R_u, \end{aligned} \quad (10)$$

where operator $\mathcal{O}_{K\bar{K}}^I$ creates a $K\bar{K}$ state with total isospin I . Since, in this paper, we preliminarily report our lattice simulations on $K\bar{K}$ scattering length in the $I = 1$ channel, in the following discussions, we will remove the superscript I for the corresponding quantities.

There are some different methods to parameterize the low-momentum behavior of the scattering amplitude. To calculate the $K\bar{K}$ scattering lengths on the lattice, we adopt the Lüscher formula, and it is straightforward to use the standard effective range expansion for the $K\bar{K}$ scattering phase shift, namely,

$$k \cot \delta_0(k) = \frac{1}{a} + \frac{1}{2} r k^2 + \mathcal{O}(k^4), \quad (11)$$

where $\delta_0(k)$ is s -wave scattering phase shift, a is the scattering length, r is the effective range, and k is the magnitude of the center-of-mass scattering momentum related to the total energy of the $K\bar{K}$ system in a cubic box of size L by $E_{K\bar{K}} = 2\sqrt{m_K^2 + k^2}$, where m_K is kaon mass. This expansion is only valid at low energy, unfortunately, takes inelasticities not into consideration.

If we approximate the $K\bar{K}$ element of the S matrix by its dominant pole contribution, the s -wave $K\bar{K}$ scattering length in the continuum is denoted by employing the standard Lüscher formula

$$a_0 = \lim_{k \rightarrow 0} \frac{\tan \delta_0(k)}{k},$$

where the scattering is purely elastic below inelastic thresholds. We should bear in mind that the truncation of the effective range r in Eq. (11) serves as a source of the systematic uncertainty, which appears as $\mathcal{O}(1/L^6)$ and in this paper we ignore it. $\delta_0(k)$ is the s -wave scattering phase shift, which can be evaluated by the Lüscher's finite size formula [23, 24],

$$\left(\frac{\tan \delta_0(k)}{k} \right)^{-1} = \frac{\sqrt{4\pi}}{\pi L} \cdot \mathcal{Z}_{00} \left(1, \frac{k^2}{(2\pi/L)^2} \right), \quad (12)$$

where the zeta function $\mathcal{Z}_{00}(1; q^2)$ is denoted by

$$\mathcal{Z}_{00}(1; q^2) = \frac{1}{\sqrt{4\pi}} \sum_{\mathbf{n} \in \mathbb{Z}^3} \frac{1}{n^2 - q^2}, \quad (13)$$

here $q = kL/(2\pi)$, and in this work the zeta function $\mathcal{Z}_{00}(1; q^2)$ is calculated by the method in Ref. [35].

The energy $E_{K\bar{K}}$ of the $K\bar{K}$ system can be obtained from the $K\bar{K}$ four-point correlator. At large t these correlators behave as [36, 37]

$$\begin{aligned} C_{K\bar{K}}(t) &= Z_{K\bar{K}} \cosh \left[E_{K\bar{K}} \left(t - \frac{T}{2} \right) \right] + \\ &(-1)^t Z'_{K\bar{K}} \cosh \left[E'_{K\bar{K}} \left(t - \frac{T}{2} \right) \right] + \dots \end{aligned} \quad (14)$$

where $E_{K\bar{K}}$ is the energy of the lightest $K\bar{K}$ state. The second term alternating in sign is a peculiarity of the staggered scheme [36, 37].

In our concrete calculation we also measure the energy shift $\delta E = E_{K\bar{K}} - 2m_K$ from the ratio

$$R^X(t) = \frac{C_{K\bar{K}}^X(0, 1, t, t+1)}{C_K(0, t)C_K(1, t+1)}, \quad X = D \text{ and } R_u, \quad (15)$$

where C_K is the kaon two-point correlator. Considering equation (10), we can write the amplitudes which project out the $I = 1$ isospin eigenstate as

$$R(t) = R^D(t) - R^{R_u}(t). \quad (16)$$

We should stress that, as compared to the contributions of the Nambu-Goldstone kaon and anti-kaon, these of the non-Nambu-Goldstone kaons and anti-kaons in the intermediate states are exponentially suppressed for large times due to their heavier masses [30, 31, 33]. In the current study we assume that the $K\bar{K}$ interpolator does not couple significantly to other $K\bar{K}$ tastes, and ignore this systematic error.

III. SIMULATION RESULTS

We calculated $K\bar{K}$ correlator on MILC lattice ensemble of 200 $16^3 \times 48$ gauge configurations with bare gauge coupling $10/g^2 = 6.572$ and bare quark masses $am_{ud}/am_s = 0.0097/0.0484$. Its physical volume is about 2.5 fm. The inverse lattice spacing $a^{-1} = 1.358_{-13}^{+35}$ GeV [28, 29] (about 0.15 fm). The dynamical strange quark mass is quite close to its physical value [28, 29].

The necessary matrix element of inverse fermion matrix are computed using the standard conjugate gradient method. We calculate the $K\bar{K}$ correlators on all the time slices for both source and sink. After averaging over all its possible values, the statistics are dramatically enhanced because we can place the kaon and anti-kaon sources at all time slices.

Using the same lattice gauge configurations, we calculate the $K\bar{K}$ four-point correlation functions with six light u valence quarks, namely, $am_x = 0.0097, 0.01067, 0.01261, 0.01358, 0.01455$ and 0.0194 , where we adopt MILC convention: m_x is the valence u/d quark mass. The strange sea quark mass is chosen at its physical number [29].

In Fig. 4 the individual ratios, R^X ($X = D$ and R_u) are shown as the functions of t for $am_x = 0.0097$. The values of the direct amplitude R^D is quite close to unity, suggesting the weak interaction in this channel. After a beginning increase up to $t \sim 4$, the rectangular amplitude shows an approximately linear decrease up until $t \sim 20$, indicating an attractive force between the kaon and anti-kaon in this channel. These features are what we expected from the theoretical predictions [33]. The systematically oscillating characteristics in the large time region is also distinctly noticed, which is a speciality of the staggered scheme [36, 37].

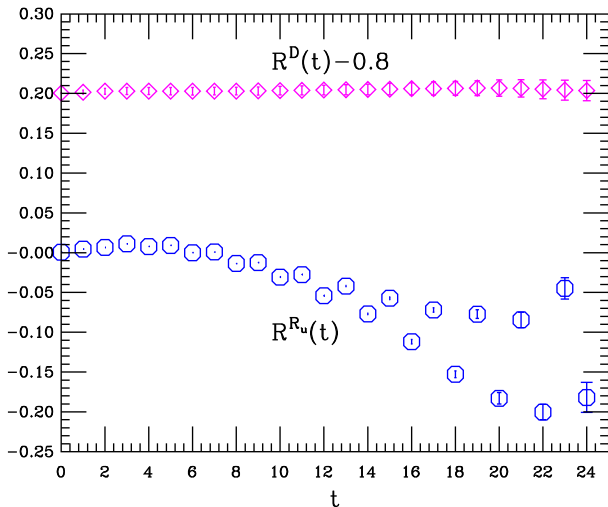


FIG. 4: Individual amplitude ratios $R^X(t)$ for $K\bar{K}$ four-point function measured by the moving wall source without gauge fixing as functions of t : Direct diagram shifted by 0.8 (diamonds) and rectangular (octagons) diagrams.

In our previous works [20, 38, 39], we have measured the pion and kaon point-to-point correlators, and calculated the pion mass m_π , kaon mass m_K , and pion decay constants f_π , which are summarized in Table I of Ref. [20]. In this work, we will directly quote these values.

According to the arguments in Ref. [40], the ratios for the rectangular R_u diagram have errors, which increase exponentially as $e^{m_\pi t}$ from large time separation². The magnitude of the errors is in quantitative agreement with this expectation as displayed in Fig. 5. Fitting the errors $\delta R^{R_u}(t)$ by a single exponential fit ansatz $\delta R^{R_u}(t) \sim e^{\mu_R t}$, we can obtain the corresponding fitting values of μ_R . The fitted values of μ_R in lattice units and

² The errors for vacuum amplitudes should be roughly independent of t , and grows exponentially as $e^{2m_K t}$ in the ratio R_V . While for the rectangular diagram R_s , it increases as $e^{m_{s\bar{s}} t}$, where $m_{s\bar{s}}$ is a fictitious meson with two valence quarks with mass about m_s . Thus, the reliable calculations of these terms are beyond the scope of this paper since it requires a substantial amount of computing resources.

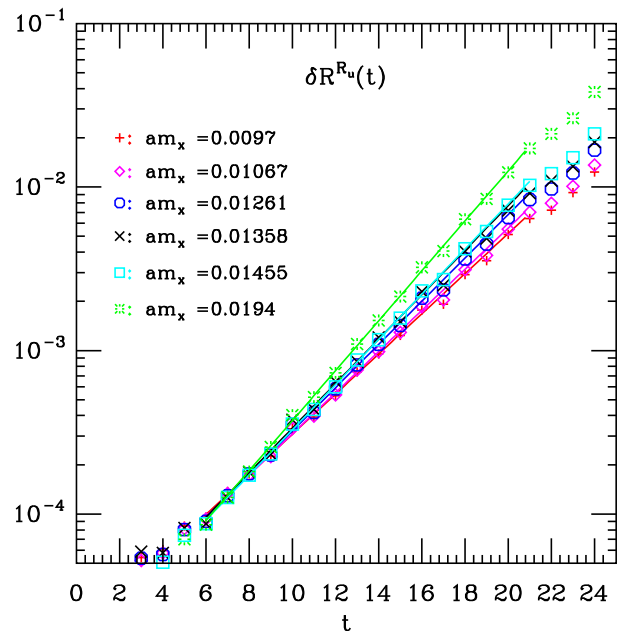


FIG. 5: The errors of the ratios $R^{R_u}(t)$ as the functions of t . Solid lines are single exponential fits.

its fitting ranges are summarized in Table I. From Table I, we can note that the fitted values of μ_R can be compared with the corresponding pion masses m_π listed in Table I of Ref. [20]. This demonstrates, on the other side, that the technique of the moving wall source without gauge fixing used in the current work for the $K\bar{K}$ scattering is practically feasible.

TABLE I: Summary of the fitted values of μ_R in lattice units. The second block shows the fitted values for μ_R , Column three shows the time range for the chosen fit.

am_x	$a\mu_R$	Range
0.0097	0.2768	8 – 14
0.01067	0.2825	8 – 14
0.01261	0.3047	8 – 14
0.01358	0.3134	8 – 14
0.01455	0.3183	8 – 14
0.0194	0.3518	8 – 14

As we practiced in Ref. [20], we understood that the correctly extracting these energies is very important to our ultimate results, and in our concrete simulation, they were chosen by searching for the combination of a “plateau” in the energy as the function of the minimum distance, and a good chi-square (namely, χ^2). In Fig. 6 we plot the $K\bar{K}$ correlation function for $am_x = 0.0097$, where we can compare the fitted functional form with the lattice data. The fitted values of the energies aE , fitting range and fitting quality are listed in Table II.

We now can plug these energies in Table II into Eq. (11) to achieve the scattering lengths. The center-of-mass scattering momentum k^2 in GeV and the scat-

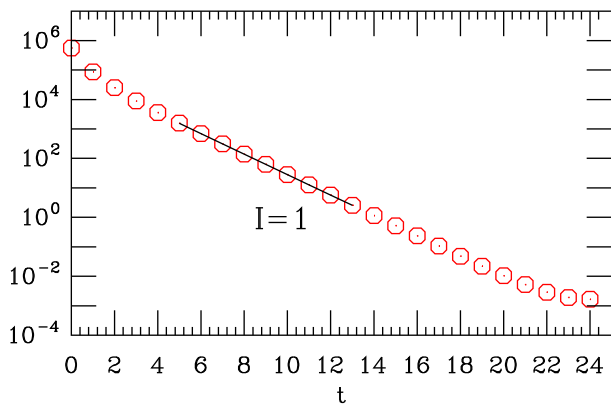


FIG. 6: The $K\bar{K}$ correlator calculated with the moving wall source without gauge fixing for $am_x = 0.0097$. Solid line is the fit for $6 \leq t \leq 12$ using the fitting model in Eq. (14).

TABLE II: Summary of the lattice results for the fitted values of the energy. The third block shows its fit range, and the fourth block gives its fit quality χ^2/dof .

am_x	aE	Range	χ^2/dof
0.00970	0.7862(6)	6 – 12	4.29/3
0.01067	0.7931(6)	6 – 12	4.81/3
0.01261	0.8071(6)	6 – 12	4.96/3
0.01358	0.8139(6)	6 – 12	5.01/3
0.01455	0.8207(6)	6 – 12	5.12/3
0.01940	0.8538(5)	6 – 12	5.58/3

tering lengths are tabulated in Table III. Here we utilize the kaon masses given in Table I of Ref. [20]. The errors of the scattering momentum k and the scattering lengths are estimated from the statistic errors of the energies E and kaon masses m_K .

TABLE III: Summary of lattice results for the scattering lengths. Column two gives the center-of-mass scattering momentum k^2 in GeV^2 , and the third block shows the kaon mass times the scattering lengths.

am_x	$k^2[\text{GeV}^2]$	$m_K a_{K\bar{K}}$
0.00970	-0.00444(54)	0.363(52)
0.01067	-0.00446(53)	0.368(52)
0.01261	-0.00451(52)	0.378(52)
0.01358	-0.00483(53)	0.414(54)
0.01455	-0.00471(54)	0.406(55)
0.01940	-0.00488(54)	0.441(58)

In Fig. 7, the s -wave $K\bar{K}$ scattering lengths $m_K a_{K\bar{K}}^{I=1}$ are displayed as a function of m_K^2 . In this work, we use pion masses $m_\pi = 330 - 466$ MeV, and need to extrapolate the $K\bar{K}$ scattering lengths toward the physical point. For this end, in B we provide the continuum $\text{SU}(3)$ χPT form at NLO for $a_{K\bar{K}}^{I=1}$, which can be directly built from

the its scattering amplitudes in Ref. [32], namely,

$$m_K a_{K\bar{K}}^{I=1} = \frac{m_K^2}{8\pi f_\pi^2} \left\{ 1 + \frac{16m_\pi^2}{f_\pi^2} L_5(\mu) + \frac{32m_K^2}{f_\pi^2} L_{K\bar{K}}^{I=1}(\mu) + \frac{1}{16\pi^2 f_\pi^2} \chi_{K\bar{K}}^{I=1}(\mu) \right\}, \quad (17)$$

where we substituted the pion mass m_π , kaon mass m_K and pion decay constant f_π listed in Table I of Ref. [20]. $L_5(\mu)$ and $L_{K\bar{K}}^{I=1}(\mu) \equiv 2L_1 + 2L_2 + L_3 - 2L_4 - \frac{1}{2}L_5 + 2L_6 + L_8$ are low-energy constants denoted in Ref. [41] and explicitly dependent on the chiral scale μ . The $\chi_{K\bar{K}}^{I=1}(\mu)$ is the known functions at NLO including chiral logarithm terms, see Eq. (B5) for details.

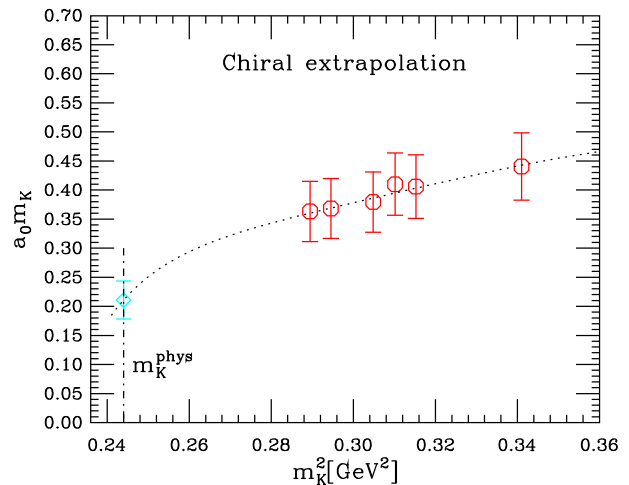


FIG. 7: m_K^2 -dependence of the $K\bar{K}$ scattering lengths $m_K a_{K\bar{K}}$ for the $I = 1$ channel. The cyan diamond point indicate its physical values.

To enhance the χPT fit, we include all the lattice simulation data of the $K\bar{K}$ scattering lengths. The fitting results of the $K\bar{K}$ scattering lengths $m_K a_{K\bar{K}}^{I=1}$ are plotted by the dotted lines as a function of m_K^2 in Fig. 7. The chirally extrapolated $K\bar{K}$ scattering length $m_K a_{K\bar{K}}^{I=1} = 0.211(33)$, the cyan diamond points in Fig. 7 demonstrates this value. The fit parameters $L_{\pi K}, L_5$, and the scattering lengths $m_K a_{K\bar{K}}^{I=1}$ at the physical points (namely, $m_\pi = 0.140$ GeV, $m_K = 0.494$ GeV) [25] are also summarized in Table IV, and the chiral scale μ is chosen as the physical η mass, namely, $\mu = 0.548$ GeV [25] as it is done in Ref. [20].

TABLE IV: The fitted s -wave scattering lengths $m_K a_{K\bar{K}}^{I=1}$ at the physical point ($m_\pi = 0.140$ GeV, $m_K = 0.494$ GeV). The chiral scale μ is taken as the physical η mass.

χ^2/dof	$10^3 \cdot L_{K\bar{K}}^{I=1}$	$10^3 \cdot L_5$	$m_K a_{K\bar{K}}^{I=1}$
0.656/4	-2.41 ± 1.10	4.90 ± 4.35	0.211 ± 0.033

From Fig. 7, we can observe that our lattice simulation results of the scattering lengths have a large error,

and are in reasonable agreement with the SU(3) χ Pt at NLO. The fitted values of the L_5 and $m_K a_{K\bar{K}}^{I=1}$ have large statistical errors, which reflect the big errors of our extracted lattice data of $m_K a_{K\bar{K}}^{I=1}$. Thus we can not claim they have physical meanings.

In this work, we only consider the statistical errors. The possible sources of the systematic errors on the extrapolated value of $m_K a_{K\bar{K}}^{I=1}$ mainly contains two parts. First, according to aforementioned discussions, when extracting $m_K a_{K\bar{K}}^{I=1}$, we ignore two major systematic errors: the truncation of the effective range r and the contributions of the non-Nambu-Goldstone kaons and anti-kaons in the intermediate states. These systematic errors of the extracting $m_K a_{K\bar{K}}^{I=1}$ should propagate through the chiral extrapolation. Second, the extrapolation to the physical point needs the experimental value for m_π , m_K and f_π . The experimental error on these quantities brings a quite small systematic error as compared to the corresponding statistical error and therefore is neglected.

IV. SUMMARY AND OUTLOOK

In this work we have carried out lattice study of $K\bar{K}$ scattering lengths, and performed a concrete lattice calculation of $K\bar{K}$ scattering lengths for isospin $I = 1$ channel, where rectangular diagram plays a vital role, for the MILC medium coarse ($a = 0.15$ fm) lattice ensemble with the Asqtad improved the staggered dynamical sea quarks. We employed the technique in Refs. [30, 31] (namely, the moving wall sources without gauge fixing) to reliably calculate $K\bar{K}$ four-point correlation function, and observed a clear signal of the attraction for isospin $I = 1$ channel, which is in well accordance with the pioneering lattice studies on $K\bar{K}$ potential in Refs. [17, 18]. Extrapolating the lattice data of the s -wave scattering lengths to the physical point, we achieved the scattering length $m_K a_{K\bar{K}}^{I=1} = 0.211(33)$ directly from lattice simulations.

A good signal can be seen for long time separation range in the rectangular R_u diagram of $K\bar{K}$ scattering. We can further reduce the noise by a larger lattice volume or smaller pion mass, and hence obtain better results for the scattering length. Moreover, as pointed above, if we want to obtain the good signals of the rectangular R_s and vacuum diagrams, we should choose lattice ensemble with suitable strange quark.

We should understand that the investigation on $K\bar{K}$ scattering at the $I = 1$ channel is just first step in the study of the $K\bar{K}$ scattering. Since the K^+K^- system is a mixture of the isospin $I = 0$ and 1, and now there are enough experimental results about its scattering lengths, the lattice study on $K\bar{K}$ scattering length at the $I = 0$ channel is highly desired. We are planning a series of lattice studies on it.

Acknowledgments

This work is supported in part by Fundamental Research Funds for the Central Universities (2010SCU23002). We thank MILC Collaboration for using their lattice ensemble. We should thank Eulogio Oset for his encouraging and constructive comments, and Zhi-Hui Guo and Hou qing for their kind helps. The computations for this work were done at AMAX, CENTOS and HP workstations in the Institute of Nuclear Science & Technology, Sichuan University.

Appendix A: $I = 1$ $K\bar{K}$ scattering amplitudes in terms of quark propagators

$$\begin{aligned} \langle O_{K^+}(x_4)O_{K^-}(x_3)O_{K^+}^\dagger(x_2)O_{K^-}^\dagger(x_1) \rangle = \\ \text{Tr} \left(G^{(u)}(x_2, x_4)\gamma_5 G^{(s)}(x_4, x_2)\gamma_5 \right) \times \\ \text{Tr} \left(G^{(u)}(x_3, x_1)\gamma_5 G^{(s)}(x_1, x_3)\gamma_5 \right) \end{aligned} \quad (\text{A1})$$

$$\begin{aligned} - \text{Tr} \left(G^{(s)}(x_2, x_4)\gamma_5 G^{(u)}(x_4, x_3)\gamma_5 \times \right. \\ \left. G^{(s)}(x_3, x_1)\gamma_5 G^{(u)}(x_1, x_2)\gamma_5 \right) \end{aligned} \quad (\text{A2})$$

$$\begin{aligned} - \text{Tr} \left(G^{(u)}(x_1, x_3)\gamma_5 G^{(s)}(x_3, x_4)\gamma_5 \times \right. \\ \left. G^{(u)}(x_4, x_2)\gamma_5 G^{(s)}(x_2, x_1)\gamma_5 \right) \end{aligned} \quad (\text{A3})$$

$$\begin{aligned} + \text{Tr} \left(G^{(u)}(x_3, x_4)\gamma_5 G^{(s)}(x_4, x_3)\gamma_5 \times \right. \\ \left. \text{Tr} \left(G^{(u)}(x_2, x_1)\gamma_5 G^{(s)}(x_1, x_2)\gamma_5 \right) \right). \end{aligned} \quad (\text{A4})$$

$$\begin{aligned} \langle O_{K^+}(x_4)O_{K^-}(x_3)O_{K^0}^\dagger(x_2)O_{\bar{K}^0}^\dagger(x_1) \rangle = \\ - \text{Tr} \left(G^{(u)}(x_3, x_4)\gamma_5 G^{(s)}(x_4, x_2)\gamma_5 \right) \times \\ \text{Tr} \left(G^{(d)}(x_2, x_1)\gamma_5 G^{(s)}(x_1, x_3)\gamma_5 \right) \end{aligned} \quad (\text{A5})$$

$$\begin{aligned} - \text{Tr} \left(G^{(s)}(x_3, x_4)\gamma_5 G^{(u)}(x_4, x_3)\gamma_5 \right) \times \\ \text{Tr} \left(G^{(s)}(x_2, x_1)\gamma_5 G^{(d)}(x_1, x_2)\gamma_5 \right). \end{aligned} \quad (\text{A6})$$

$$\begin{aligned} \langle O_{K^0}(x_4)O_{\bar{K}^0}(x_3)O_{K^+}^\dagger(x_2)O_{\bar{K}^-}^\dagger(x_1) \rangle = \\ - \text{Tr} \left(G^{(d)}(x_3, x_4)\gamma_5 G^{(s)}(x_4, x_2)\gamma_5 \right) \times \\ \text{Tr} \left(G^{(u)}(x_2, x_1)\gamma_5 G^{(s)}(x_1, x_3)\gamma_5 \right) \end{aligned} \quad (\text{A7})$$

$$\begin{aligned} - \text{Tr} \left(G^{(d)}(x_3, x_4)\gamma_5 G^{(s)}(x_4, x_3)\gamma_5 \right) \times \\ \text{Tr} \left(G^{(u)}(x_2, x_1)\gamma_5 G^{(s)}(x_1, x_2)\gamma_5 \right). \end{aligned} \quad (\text{A8})$$

$$\begin{aligned} \langle O_{K^0}(x_4)O_{\bar{K}^0}(x_3)O_{K^0}^\dagger(x_2)O_{\bar{K}^0}^\dagger(x_1) \rangle = \\ \text{Tr} \left(G^{(d)}(x_2, x_4)\gamma_5 G^{(s)}(x_4, x_2)\gamma_5 \right) \times \end{aligned}$$

$$\text{Tr} \left(G^{(d)}(x_3, x_1) \gamma_5 G^{(s)}(x_1, x_3) \gamma_5 \right) \quad (\text{A9})$$

$$- \text{Tr} \left(G^{(d)}(x_2, x_4) \gamma_5 G^{(s)}(x_4, x_3) \gamma_5 \times \right. \\ \left. G^{(d)}(x_3, x_1) \gamma_5 G^{(s)}(x_1, x_2) \gamma_5 \right) \quad (\text{A10})$$

$$- \text{Tr} \left(G^{(d)}(x_3, x_4) \gamma_5 G^{(s)}(x_4, x_2) \gamma_5 \times \right. \\ \left. G^{(d)}(x_2, x_1) \gamma_5 G^{(s)}(x_1, x_2) \gamma_5 \right) \quad (\text{A11})$$

$$+ \text{Tr} \left(G^{(s)}(x_3, x_4) \gamma_5 G^{(d)}(x_4, x_3) \gamma_5 \right) \times \\ \text{Tr} \left(G^{(s)}(x_2, x_1) \gamma_5 G^{(d)}(x_1, x_2) \gamma_5 \right). \quad (\text{A12})$$

Appendix B: The analytic expression of s -wave $K\bar{K}$ scattering length for the isospin $I = 1$ channel

In the isospin limit, both isospin amplitudes in $K\bar{K} \rightarrow K\bar{K}$ can be described by two independent amplitudes T_{ch} (the amplitude for the processes $K^+K^- \rightarrow K^+K^-$) and T_{neu} (that for $\bar{K}^0K^0 \rightarrow K^+K^-$) [1, 11, 16]. Z. H. Guo and J. A. Oller derived two isospin amplitudes only in terms of T_{neu} [32]. Here we follow the notations and conventions in [32], since the the chiral scale μ dependence in amplitude is canceled by the loops and the low energy constants (LECs) [32].

These amplitudes can be decomposed into partial waves $t_l(s)$ according to

$$T(s, t, u) = 16\pi \sum_l (2l+1) t_l(s) P_l(\cos \theta),$$

where l is total angular momentum, θ denotes scattering angle in the center-of-mass system. In the elastic region, the partial wave amplitude $t_l(s)$ can be parameterized by real phase shifts $\delta_l(s)$,

$$t_l^I(s) = \sqrt{\frac{s}{s-4m_K^2}} \frac{1}{2i} \left\{ e^{2i\delta_l^I(s)} - 1 \right\}.$$

And its real part can be expanded at threshold (namely, $s = 4m_K^2, t = 0, u = 0$) in terms of the scattering lengths ($a_l^{I=1}$) and effective ranges ($b_l^{I=1}$),

$$\text{Re } t_l^I(s) = \frac{\sqrt{s}}{2} q^{2l} \left\{ a_l^{I=1} + b_l^{I=1} q^2 + \mathcal{O}(q^4) \right\},$$

for the center-of-mass three-momentum of the kaons q . The s -wave scattering length is linked to the real part of the amplitude at threshold by

$$\text{Re } T_{\text{thr}}^{I=1} = 16\pi m_K a_{K\bar{K}}^{I=1} + \mathcal{O}(q^2).$$

The one-loop order analytic expressions of $K\bar{K}$ scattering amplitudes in the isospin limit can be found in Ref. [32], however, no analytic formulae for s -wave scattering lengths were explicitly provided. We, therefore, will present it for isospin $I = 1$ channel. To this end,

we first expand the scattering amplitude at threshold, namely³,

$$T(s, t, u) = \frac{2m_K^2}{f_\pi^2} + \frac{32m_K^2 m_\pi^2}{f_\pi^4} L_5(\mu) + \frac{64m_K^4}{f_\pi^4} L_{K\bar{K}}^{I=1}(\mu) \\ - \frac{(3m_\eta^2 + m_\pi^2)^2 + 144m_K^4}{288\pi^2 f_\pi^4} - \frac{3m_K^4}{8\pi^2 f_\pi^4} \log \frac{m_K^2}{\mu^2} \\ + \frac{1}{432\pi^2 f_\pi^4 (m_\eta^2 - m_\pi^2)} \left[m_\pi^2 (376m_K^4 + 100m_K^2 m_\pi^2) \right. \\ \left. + m_\pi^4 - 228m_\eta^2 m_K^2 + 3m_\eta^2 m_\pi^2 \right] \log \frac{m_\pi^2}{\mu^2} \\ + \frac{1}{4320\pi^2 f_\pi^4 (m_\eta^2 - m_\pi^2)} \left[15m_\pi^6 - 441m_\eta^6 \right. \\ \left. + 3m_\eta^4 (716m_K^2 + 73m_\pi^2) \right. \\ \left. + m_\eta^2 (167m_\pi^4 - 3760m_K^4 - 868m_\pi^2 m_K^2) \right] \log \frac{m_\eta^2}{\mu^2} \\ + \bar{J}_{KK}(s = 4m_K^2) \frac{4m_K^4}{f_\pi^4} \\ + \bar{J}_{\pi\eta}(s = 4m_K^2) \frac{(3m_\eta^2 - 28m_K^2 + m_\pi^2)^2}{54f_\pi^4}, \quad (\text{B1})$$

where $L_{K\bar{K}}^{I=1}(\mu) \equiv 2L_1 + 2L_2 + L_3 - 2L_4 - \frac{1}{2}L_5 + 2L_6 + L_8$ are low-energy constants defined in Ref. [41] at the chiral symmetry breaking scale μ . The loop function \bar{J}_{PQ} is given in Ref. [41], namely,

$$\bar{J}_{\pi\eta}(s = 4m_K^2) = \frac{1}{32\pi^2} \left\{ 2 + \left(\frac{m_\pi^2 - m_\eta^2}{4m_K^2} - \frac{m_\pi^2 + m_\eta^2}{m_\pi^2 - m_\eta^2} \right) \ln \frac{m_\eta^2}{m_\pi^2} \right. \\ \left. - \frac{\nu}{4m_K^2} \ln \frac{(4m_K^2 + \nu)^2 - (m_\pi^2 - m_\eta^2)^2}{(4m_K^2 - \nu)^2 - (m_\pi^2 - m_\eta^2)^2} \right\}, \quad (\text{B2})$$

with $\nu = \sqrt{[4m_K^2 - (m_\pi + m_\eta)^2][4m_K^2 - (m_\pi - m_\eta)^2]}$

. By plugging the leading order relation $m_\eta^2 = (4m_K^2 - m_\pi^2)/3$ [32] we can simplify the above formula as

$$T(s, t, u) = \frac{2m_K^2}{f_\pi^2} + \frac{32m_K^2 m_\pi^2}{f_\pi^4} L_5(\mu) + \frac{64m_K^4}{f_\pi^4} L_{K\bar{K}}^{I=1}(\mu) \\ - \frac{5m_K^4}{9\pi^2 f_\pi^4} - \frac{3m_K^4}{8\pi^2 f_\pi^4} \log \frac{m_K^2}{\mu^2} \\ + \frac{m_\pi^2 m_K^2 (2m_K^2 + 5m_\pi^2)}{16\pi^2 f_\pi^4 (m_K^2 - m_\pi^2)} \log \frac{m_\pi^2}{\mu^2} \\ + \frac{9m_\pi^4 m_K^2 - 16m_K^4 m_\pi^2 - 56m_K^6}{144\pi^2 f_\pi^4 (m_K^2 - m_\pi^2)} \log \frac{4m_K^2 - m_\pi^2}{3\mu^2} \\ + \bar{J}_{KK}(s = 4m_K^2) \frac{4m_K^4}{f_\pi^4}$$

³ Zhi-Hui Guo kindly give the following formulae to me to fitting our lattice data. In there, we especially thank him. Without his kind help, we can not finish this work smoothly. Nevertheless, in this work, we use $f_\pi = 132\text{MeV}$ instead of 93 MeV in Guo's original formula.

$$+\bar{J}_{\pi\eta}(s=4m_K^2)\frac{32m_K^4}{3f_\pi^4}. \quad (\text{B3})$$

And the scattering length can be written in a compact form,

$$a_{K\bar{K}}^{I=1} = \frac{m_K}{8\pi f_\pi^2} \left\{ 1 + \frac{16m_\pi^2}{f_\pi^2} L_5(\mu) + \frac{32m_K^2}{f_\pi^2} L_{K\bar{K}}^{I=1}(\mu) + \frac{1}{(4\pi f_\pi)^2} \chi_{K\bar{K}}^{I=1}(\mu) \right\}, \quad (\text{B4})$$

where $\chi_{K\bar{K}}^{I=1}(\mu)$ is the known functions at NLO which

$$\begin{aligned} \chi_{K\bar{K}}^{I=1}(\mu) = & -3m_K^2 \ln \frac{m_K^2}{\mu^2} + \frac{m_\pi^2}{2} \frac{2m_K^2 + 5m_\pi^2}{m_K^2 - m_\pi^2} \ln \frac{m_\pi^2}{\mu^2} \\ & + \frac{9m_\pi^4 - 16m_K^2 m_\pi^2 - 56m_K^4}{18(m_K^2 - m_\pi^2)} \log \frac{4m_K^2 - m_\pi^2}{3\mu^2} \\ & - \frac{4}{9} m_K^2 + \bar{J}_{\pi\eta}(s=4m_K^2) \frac{256\pi^2 m_K^2}{3}. \end{aligned} \quad (\text{B5})$$

-
- [1] J. A. Oller, E. Oset and J. R. Pelaez, Phys. Rev. D **59**, 074001 (1999). arXiv:hep-ph/9804209
- [2] P. Winter et al., Phys. Lett. B **635**, 23 (2006). arXiv:hep-ex/0602030
- [3] Y. Maeda et al. [The ANKE Collaboration], Phys. Rev. C **77**, 015204 (2008). arXiv:0710.1755 [nucl-ex]
- [4] A. Dzyuba et al., Phys. Lett. B **668**, 315 (2008). arXiv:0807.0524 [nucl-th]
- [5] Y. Maeda et al., Phys. Rev. C **79**, 018201 (2009). arXiv:0811.4303 [nucl-ex]
- [6] M. Silarski et al. [COSY-11 collaboration], Phys. Rev. C **80**, 045202 (2009). arXiv:0909.3974 [hep-ph]
- [7] J. J. Xie and C. Wilkin, Phys. Rev. C **82**, 025210 (2010). arXiv:1005.2957 [nucl-th]
- [8] B. Lorentz et al., J. Phys. Conf. Ser. **295**, 012146 (2011)
- [9] M. Silarski, Int. J. Mod. Phys. A **26**, 539 (2011). arXiv:1008.3620 [hep-ph]
- [10] N.N. Wong and A.N. Kamal, Phys. Rev. D **11**, 1896 (1975)
- [11] F. Guerrero and J. A. Oller, Nucl. Phys. B **537**, 459 (1999). arXiv:hep-ph/9805334
- [12] R. W. Griffith, Phys. Rev. **176**, 1705 (1968)
- [13] J.A. Oller and E. Oset, Nucl. Phys. A **620**, 438 (1997)
- [14] J.A. Oller and E. Oset, Phys. Rev. D **60**, 074023 (1999). hep-ph/9809337
- [15] M. Doring, U.G. Meissner, E. Oset and A. Rusetsky, Eur. Phys. J. A **47**, 139 (2011). arXiv:1107.3988 [hep-lat].
- [16] A. Gomez Nicola and J.R. Pelaez, Phys. Rev. D **65**, 054009 (2002). arXiv:hep-ph/0109056
- [17] A. Mihály, “Studies of Meson-Meson Interactions within Lattice QCD”, PhD thesis, Lajos Kossuth University, Debrecen, 1998
- [18] A. Mihaly, H. R. Fiebig, H. Markum and K. Rabitsch, Heavy Ion Phys. **9**, 349 (1999).
- [19] S. R. Beane et al., Phys. Rev. D **77**, 094507 (2008). arXiv:0709.1169 [hep-lat]
- [20] Z. Fu, Phys. Rev. D **85**, 074501 (2012). arXiv:1110.1422 [hep-lat]
- [21] Z. Fu, JHEP **01**, 017 (2012). arXiv:1110.5975 [hep-lat]
- [22] Z. Fu, Commun. Theor. Phys. **57**, 78 (2012). arXiv:1110.3918 [hep-lat]
- [23] M. Luscher, Nucl. Phys. B **354**, 531 (1991)
- [24] L. Lellouch and M. Luscher, Commun. Math. Phys. **219** 31 (2001)
- [25] K. Nakamura et al., J. Phys. G **37**, 075021 (2010)
- [26] K. Orginos and D. Toussaint [MILC Collaboration], Phys. Rev. D **59**, 014501 (1998)
- [27] K. Orginos, D. Toussaint and R. L. Sugar [MILC Collaboration], Phys. Rev. D **60**, 054503 (1999)
- [28] C. Bernard et al., Phys. Rev. D **83**, 034503 (2011)
- [29] A. Bazavov et al., Rev. Mod. Phys. **82**, 1349 (2010)
- [30] Y. Kuramashi, M. Fukugita, H. Mino, M. Okawa and A. Ukawa, Phys. Rev. Lett. **71** 2387 (1993)
- [31] M. Fukugita, Y. Kuramashi, M. Okawa, H. Mino and A. Ukawa, Phys. Rev. D **52**, 3003 (1994)
- [32] Z.H. Guo and J.A. Oller, Phys. Rev. D **84**, 034005 (2011)
- [33] S. R. Sharpe, R. Gupta and G. W. Kilcup Nucl. Phys. B **383**, 309 (1992)
- [34] J. Nagata, S. Muroya, A. Nakamura, Phys. Rev. C **80**, 045203 (2009)
- [35] T. Yamazaki et al., Phys. Rev. D **70**, 074513 (2004)
- [36] D. Barkai, K. J. M. Moriarty and C. Rebbi, Phys. Lett. B **156**, 385 (1985)
- [37] A. Mihaly, H. R. Fiebig, H. Markum and K. Rabitsch, Phys. Rev. D **55**, 3077 (1997)
- [38] Z. Fu, Chin. Phys. Lett. **28**(8), 081202 (2011)
- [39] Z. Fu, Chin. Phys. C **37**, 1079 (2011)
- [40] G. P. Lepage, in Proceedings of TASI’89 Summer School, edited by T. DeGrand and D. Toussaint (World Scientific, Singapore, 1990), p. 97
- [41] J. Gasser and H. Leutwyler, Nucl. Phys. **B250**, 465 (1985)